New sodalite frameworks; synthetic tugtupite and a beryllosilicate framework with a 3 : 1 Si : Be ratio†

J. A. Armstrong and M. T. Weller

Received 13th January 2006, Accepted 2nd March 2006
First published as an Advance Article on the web 16th March 2006
DOI: 10.1039/b600579a

Compounds of the formula $Na_8[Si_{6+y}Be_yAl_{6-2y}O_{24}]X_2$, with X = Cl and Br, and $y = 1$, 2 and 3 have been synthesised and structurally characterised by combined powder X-ray and neutron diffraction profile analysis. These materials adopt the sodalite framework (SOD) with the tetrahedral species, BeO_4, AlO_4 and SiO_4, disordered across the framework positions. $Na_8[Si_8Be_2Al_2O_{24}]Cl_2$, ($y = 2$), is a synthetic analogue of the naturally occurring semi-precious gemstone tugtupite, while $Na_8[Si_9Be_3O_{24}]X_2$, X = Cl and Br represents a new tetrahedral framework stoichiometry with a Si : Be ratio of 3 : 1. Additional characterisation using ^{29}Si MASNMR, IR spectroscopy and high-temperature, neutron diffraction show that the observed structure–property trends found when modelling sodalite materials can be extended to these new framework compositions.

Introduction

Semi-condensed zeolite structure types lie on the border between the true porous frameworks of zeolites and the denser structures of many aluminosilicates such as the feldspathoids.[1] Among the enormous family of zeolites and zeotypes only a few structures can be synthesised with an aluminium to silicon ratio of 1 : 1 or above; these examples include zeolite A (LTA), sodalite (SOD), cancrinite (CAN), zeolite P (GIS) and zeolite X (FAU).[2–5] The difficulty in incorporating high levels of lower charged species (2+ and 3+) onto the tetrahedral framework sites (T-sites) presumably results from the weaker T–O interactions (mitigating against the formation of T–O–T links in aqueous solution, Lowenstein's rule) and the need to charge balance the structure with high levels of extra-framework cations. Significant levels of trivalent T-site ions are more common in the feldspathoid family of compounds, which are anhydrous, non porous framework aluminosilicates of the alkali/alkaline earth metals, such as nepheline, $(Na,K)AlSiO_4$.[6] Zeotype structures that contain significant levels of divalent cations in the framework are even rarer because of the need to charge balance the $[A(O_4)_{1/2}]^{2-}$ unit. Thus, beryllium-containing zeotypes are limited to those that also contain the effectively positively charged, vertex-sharing, tetrahedral $[P(O_4)_{1/2}]^+$ unit (with its strong balancing effect on the overall framework charge), Nabesite, $Na_8(H_2O)_{16}[Be_4Si_{16}O_{40}]$ (NAB),[7] with a low level of beryllium, and some members of the sodalite family.[2]

Structures containing strongly negatively charged frameworks and high levels of compensating extra-framework cations are of interest for a number of reasons. These include existing applications as ion exchangers, the potential to produce high numbers of Brønsted acid sites for catalysis and, more unusually, the ability of the high levels and densities of extra-framework cations to stabilise extra-framework anion incorporation. This latter behaviour is seen in materials such as those of the sodalite family and in the mineral kalborsite, $K_6Al_4Si_6O_{20}{\cdot}B(OH)_4{\cdot}Cl$.[8] Sodalites can be described by the general formula $M_8[ABO_4]_6{\cdot}X_2$, where M is a mono or divalent ion such as Na^+, Li^+, Ag^+, Ca^{2+},[9,10] A and B are tetrahedral forming species, such as Al or Si, and X can be a variety of mono or divalent anions, including Cl, Br, I,[11,12] $(ClO_3)^-$,[13] $(MnO_4)^-$,[14] and $1/2(CrO_4)^{2-}$.[15] The structure is based upon a truncated octahedral cage linked in three dimensions,[9] yielding four and six-membered rings that are directly linked to form the overall structure, Fig. 1. Compositional variations are numerous within this basic structure type and include additional trapped anions, such as in bicchulite, $Ca_8[Si_4Al_8O_{24}]{\cdot}(OH)_8$,[16] and $Nd_4[Al_{12}O_{24}](Pb_4O_4)_2$.[17] Gallium can totally replace aluminium, and germanium can supplant silicon, in the framework and together these substitutions give rise to frameworks of formulae $(GaSiO_4)_6^{6-}$,[18] $(AlGeO_4)_6^{6-}$,[19] and $(GaGeO_4)_6^{6-}$.[20] Incorporation of divalent species such as Be^{2+}, Mg^{2+} or Zn^{2+}[20,21] instead of Al^{3+} leads to an increased negative charge on the framework, which is normally compensated for by the inclusion of divalent non-framework cations, such as Ca^{2+}, Zn^{2+} and Fe^{2+}, giving rise to stoichiometries such as $Ca_8[BeSiO_4]_6(SO_4)_2$ and the naturally occurring minerals helvite, danalite and genthelvite, $(Fe,Zn,Mn)_8[Be_6Si_6O_{24}]S_2$.[22]

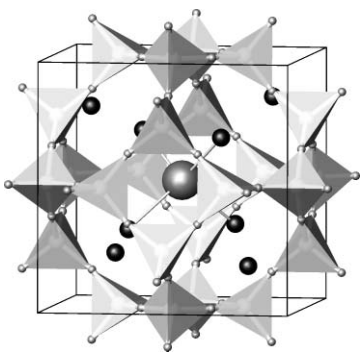

Fig. 1 The $M_8[TO_2]_{12}X_2$ sodalite framework represent as linked TO_4 tetrahedra surrounding cations M (small black spheres) and anions X (large grey spheres).

School of Chemistry, University of Southampton, Southampton, UK SO17 1BJ

† Electronic supplementary information (ESI) available: Table S1. See DOI: 10.1039/b600579a

In terms of applications, it is the optical properties of certain sodalites that have led to their exploitation as pigments, jewellery and fluorescent materials. Ultramarine blue, $Na_{8-x}[AlSiO_4]_6(S_3,S_2,SO_4,Cl\cdots)$ is used extensively as a pigment in cosmetics and plastics and its chemistry and applications have recently been reviewed.[23] There are several forms of ultramarine, containing sulfur in various polyanionic forms; the yellow, green, blue, pink, red and violet colours of various ultramarines have all been reported as being caused by polysulfide radical species S_n^- entrapped in the sodalite cages. Since disorder of the framework silicon and aluminium occurs in the man-made pigment, these compounds adopt the space group $I\bar{4}3m$ rather than $P\bar{4}3n$ of the ordered aluminosilicate sodalites, with alternating AlO_4 and SiO_4 tetrahedra.

Fluorescent properties are exhibited by many sulfur-containing sodalites following excitation by either short wave radiation or by electron beams; for example, cathodochromic properties have been reported by Chang.[24] Reversible photochromism is also found in some sodalites including the naturally occurring hackmanites, $Na_8[AlSiO_4]_6(S_2,Cl)$.[25] One of the more unusual minerals from the sodalite family is tugtupite of general formula $Na_8[Al_2Be_2Si_8O_{24}](Cl,S_n)_2$.[26] This material may occur in white, pink, red, or very rarely blue, forms and all show strong red fluorescence when excited with UV radiation. Fascinatingly pink and red forms of tugtupite reversibly darken on exposure to daylight or UV light yielding dark red/purple coloured material. This property coupled to the attractive nature of highly crystalline tugtupite has led to its use as a semi-precious gemstone in jewellery.[27]

Tugtupite is unusual as a zeotype in that involves BeO_4 tetrahedra in the construction of its framework. A few other zeolite framework types contain BeO_4 tetrahedra but generally only in combination with the charge-balancing phosphate; these include the structure codes ABW, BPH, CHA GIS, GME, LOS, MER, RHO and FAU.[28–32] In the naturally occurring Nabesite (NAB), $Na_2BeSi_4O_{10}\cdot 4H_2O$, each BeO_4 unit in the framework is linked through four silicate tetrahedra.[7]

Until now the synthesis of beryllium containing sodalites has been limited to the aforementioned systems with the framework stoichiometries $[TBeO_4]^{2-/1-}$, T = P, Si and no berylloaluminosilicate framework, synthetic equivalent of tugtupite or beryllosilicate framework with a Si : Be ratio of 3 : 1 has been reported. In this article we describe the synthesis and structural characterisation of a range of new berylloaluminosilicate sodalites of the general formula $Na_8[Si_{6+y}Be_yAl_{6-2y}O_{24}]X_2$, with X = Cl, Br and y = 1, 2 and 3, including a synthetic tugtupite and a new zeotype framework composition, $[BeSi_3O_8]^{2-}$.

Experimental

Various routes to synthetic berylloaluminosilicate sodalites were investigated including the direct reaction of the oxides with different sodium sources and reactions of pre-formed sodium aluminate/beryllate/silicates in similar mixtures. The successful route to the new sodalite framework materials used a two-stage process. The initial step involved the synthesis of a sodium silicate glass of required Na_2O : SiO_2 stoichiometry, *i.e.* $Na_6Si_7O_{17}$, $Na_6Si_8O_{19}$ and $Na_6Si_9O_{21}$, for the preparation of $Na_8[Si_7BeAl_4O_{24}]Cl_2$, $Na_8[Si_8Be_2Al_2O_{24}]Cl_2$ and $Na_8[Si_9Be_3O_{24}]Cl_2$, respectively. These glasses were synthesised by heating Na_2CO_3 and SiO_2 [Aldrich, 99.995+%], both previously dried, in the correct stoichiometry, in a platinum crucible at 1000 °C for 48 h. The glass was then removed from the crucible and ground to a fine powder and used as a starting material in the next step. The sodium silicate glass powder was ground together with stoichiometric quantities of BeO [Aldrich, 99.98%]‡ and Al_2O_3 [Aldrich 99.99%] and a four-fold excess of dried NaCl. The mixture was loaded into a silica glass ampoule, sealed under vacuum and heated at 800 °C for 48 h. The product was recovered and washed with warm distilled water to remove excess NaCl and then dried at 110 °C. All products were initially characterised by powder X-ray diffraction using a Siemens D5000 ($CuK_{\alpha 1}$ radiation) to check phase purity. Further high quality X-ray diffraction sets, with data collection times of 14 h over the angular range 15–90°, were obtained for full profile analysis.

Powder neutron diffraction data were initially collected on $Na_8[Si_8Be_2Al_2O_{24}]Cl_2$ (synthetic tugtupite) and $Na_8[Si_8Be_2Al_2O_{24}]$-Br_2 (Br-analogue of synthetic tugtupite) on the HRPD instrument, ISIS. Subsequent diffraction data were obtained from $Na_8[Si_7BeAl_4O_{24}]Cl_2$, $Na_8[Si_7BeAl_4O_{24}]Br_2$, $Na_8[Si_9Be_3O_{24}]Cl_2$, and $Na_8[Si_9Be_3O_{24}]Br_2$ on the D2B instrument, ILL. Data were initially collected at room temperature on all compositions with further data sets collected at selected higher temperatures on specific phases as follows: $Na_8[Si_8Be_2Al_2O_{24}]Cl_2$ 200, 400, 600 and 800 °C; $Na_8[Si_7BeAl_4O_{24}]Cl_2$ and $Na_8[Si_7BeAl_4O_{24}]Br_2$ 600 °C, and $Na_8[Si_9Be_3O_{24}]Cl_2$ at 300 and 600 °C.

IR spectra were recorded on Perkin Elmer Spectrum One FT-IR Spectrometer. ^{29}Si MASNMR data were collected on Bruker Avance 500 spectrometer with 4 mm MAS BB H1 probe in a zirconia rotor spinning at 12 kHz with a 1.5 microsecond pulse width and a 20 second relaxation delay; 256 scans were co-added to produce the spectrum. Data were referenced to 1 M TMS in C_6D_6 at 0 ppm.

Results

Several new beryllium containing sodalites were successfully formed in this study. Reactions in the system Na_2O : Al_2O_3 : SiO_2 : BeO : NaCl/NaBr yielded products with powder X-ray diffraction patterns containing reflections fully consistent with a cubic sodalite framework of dimensions 8.5–9 Å. Products from some reaction conditions and times were impure and contaminated with low levels of starting materials and other known phases from this system. Most prevalent was a synthetic analogue of the mineral chkalovite, $Na_6Be_3(Si_6O_{18})$,[33] though the use of excess sodium halide in the reaction mixture mitigated

‡ BeO. Beryllium compounds are toxic by inhalation and ingestion, a probable human carcinogen, may be harmful by skin contact and are a serious respiratory irritant. Acute berylliosis can develop at levels ranging from 2–1000 μg Be m^{-3} and chronic berylliosis can develop from prolonged exposure. These toxicities, while not significantly different from many commonly used chemicals, were addressed by handling the readily aerially-dispersed BeO in a glove box. Reactant compositions were weighed and ground together in a nitrogen filled glove box, placed directly in the silica ampoule and then transferred immediately to a vacuum line to be sealed. Once reacted to form the beryllosilicate frameworks the potential for inhaling beryllium is negated; however materials were still handled with sealed apparatus wherever possible to guard against the presence of any residual BeO.

against the presence of this phase. Successful syntheses of pure and near pure material were achieved under the conditions stated in the Experimental section with the powder X-ray diffraction data from these products showing a single or vast majority phase indexable on a cubic unit cell. Initial modelling of the data was undertaken using the higher quality powder X-ray data with Rietveld profile analysis, but these data were found to be relatively insensitive to some atomic positions and atom distributions, especially beryllium, and therefore powder neutron diffraction data were also obtained on each of the phases.

Full structure refinement was thus carried out by combined analysis of the X-ray and neutron diffraction data allowing more stable definition of the crystallographic model. In each case the diffraction data could be indexed on a cubic unit cell in the space group $I\bar{4}3m$. A description in this space group represents a framework in which the three tetrahedral species, Be, Al, Si, are fully disordered and contrasts with many simple aluminosilicate sodalites, which have ordered frameworks constructed from alternating SiO_4 and AlO_4 tetrahedra and are described by the space group $P\bar{4}3n$. Disordered frameworks have been reported for some aluminosilicate sodalites synthesised at high temperature including ultramarine and iodosodalite.[34,35]

Refinements proceeded smoothly with the introduction of positional and thermal displacement parameters. Various models were investigated and the final model adopted included all refineable positional variables, isotropic thermal displacement parameters for all atoms except sodium for which anisotropic displacement was included where possible. The local static disorder of sodium, which presumably results from the variability in its coordination to the disordered framework TO_4 units, is well modelled by high thermal displacement parameters. Attempts to model the local environment using multiple sodium sites were unsuccessful and the large thermal displacement parameters presented are representative of the large static disorder in this atom's position. Site occupancy factors for the non-framework atoms were varied but showed no significant shift from unity and therefore all sites were maintained at complete occupancy during the final stages of the refinement. In some cases (*e.g.* $Na_8[Si_9Be_3O_{24}]Cl_2$) a few small areas of the profile containing the strongest reflections ($I/I_0 < 0.1$) from chkalovite type phases, were placed in excluded regions—most reflections from this complex structure were very weak and modelling of this contribution as a second phase unnecessary. Final extracted structural parameters are summarised in Tables 1 and 2 together with derived bond distances and angles of importance. Fig. 2 shows an example of a final, dual-profile fit achieved.

For the neutron diffraction data collected at high temperature, from the synthetic tugtupite analogue $Na_8[Si_8Be_2Al_2O_{24}]Cl_2$ and several of the other phases, Rietveld analyses were undertaken in a similar manner, but using the neutron diffraction data alone. Extracted profile fit and structural data are summarised in the electronic supplementary information (ESI), Table S1.‡

Structural results

Analysis of the extracted structural information for the series of compounds $Na_8[Si_{6+y}Be_yAl_{6-2y}O_{24}]X_2$, X = Cl, Br and y = 1, 2, 3, shows the expected behaviours and trends based on the relative sizes of the framework cations and extra-framework anion (cationic radii in four-fold coordination, Be^{2+}, Si^{4+} and Al^{3+}, 0.27, 0.26, 0.39 Å respectively and anionic radii in six-fold coordination (no reliable datum exists for four-fold coordination), Cl^- and Br^- 1.81 and 1.96 Å). Fig. 3 shows the variation of the lattice parameter as a function of y in $Na_8[Si_{6+y}Be_yAl_{6-2y}O_{24}]X_2$, X = Cl and Br. Replacement of aluminium by beryllium and silicon on the basis 2Al = Si + Be leads to a smooth contraction in lattice parameter for both series of compounds with the drop most significant for the initial introduction of beryllium into the framework. The lattice parameter of $Na_8[Si_9Be_3O_{24}]Cl_2$ at 8.659 Å represents one of the smallest known sodalite cage sizes, particularly with extra-framework sodium; smaller cage sizes are found but only with *lithium* aluminosilicate sodalites *e.g.* $Li_8[AlSiO_4]_6Cl_2$ at 8.444 Å[31] and borate sodalites *e.g.* $Zn_4[B_6O_{12}]O$, with a = 7.478 Å.[32]

Table 1 Key crystallographic data and extracted distances/angles for $Na_8[Si_{6+y}Be_yAl_{2-y}O_{24}]Cl_2$ phases. Space group $I\bar{4}3m$. E.s.d.s. given in parentheses

	$Na_8[Be_3Si_9O_{24}]Cl_2$	$Na_8[Al_2Be_2Si_8O_{24}]Cl_2$ (HRPD)	$Na_8[Al_4BeSi_7O_{24}]Cl_2$	$Na_8[Al_6Si_6O_{24}]Cl_2$[a] ($P\bar{4}3n$)
a/Å	8.65952(28)	8.71403(8)	8.7453(4)	8.8812(3)
Atomic coordinates				
Na (8c) x	0.1785(9)	0.1841(8)	0.1841(8)	0.1777(5) [8e]
O (24g) x	0.35391(6)	0.35958(17)	0.35395(30)	0.3605(3)/0.3506(3) [24i]
z	0.0416(6)	0.04770(17)	0.04637(26)	0.0618(2) [24i]
Thermal displacement parameters $U_i/U_{eq} \times 100$/Å^2				
T	5.30(34)	0.74(7)	5.89(19)	—
O	1.78(15)	0.61(5)	2.85(7)	—
Na	8.15[b]	17.63[c]	14.34[d]	—
Cl	1.51(33)	1.67(11)	3.03(18)	—
Derived bond lengths/angles				
Na–Cl/Å	2.677(14)	2.778(12)	2.788(13)	2.734(8)
Na–O/Å	2.454(9)	2.468(6)	2.422(6)	2.3881(18)
	3.170(9)	3.214(6)	3.203(6)	3.0492(8)
T–O/Å	1.5937(18)	1.6068(5)	1.6193(9)	
T–O–T/°	147.7(4)	146.95(11)	145.38(21)	138.777

[a] Data taken from the Inorganic Chemical Structural Database. [b] Anisotropic thermal displacement parameters modelled with U_{eq} values given and refined values (U_{11}, $U_{22}\cdots$) ×100 as 8.1(6) 8.1(6) 8.1(6) 1.2(7) 1.2(7) 1.2(7). [c] Anisotropic thermal displacement parameters modelled with U_{eq} values given and refined values (U_{11}, $U_{22}\cdots$) ×100 as 17.6(7) 17.6(7) 17.6(7) −4.6(6) −4.6(6) −4.6(6). [d] Anisotropic thermal displacement parameters modelled with U_{eq} values given and refined values (U_{11}, $U_{22}\cdots$) ×100 as 14.3(6) 14.3(6) 14.3(6) 0.7(6) 0.7(6) 0.7(6).

Table 2 Key crystallographic data and extracted distances/angles for $Na_8[Si_{6+y}Be_yAl_{2-y}O_{24}]Br_2$ phases. Space group $I\bar{4}3m$. E.s.d.s. given in parentheses

	$Na_8[Be_3Si_9O_{24}]Br_2$	$Na_8[Al_2Be_2Si_8O_{24}]Br_2$ (HRPD)	$Na_8[Al_4BeSi_7O_{24}]Br_2$	$Na_8[Al_6Si_6O_{24}]Br_2$[a] ($P\bar{4}3n$)
a/Å	8.7153(6)	8.75410(11)	8.79348(6)	8.9304(3)
Atomic coordinates				
Na (8c) x	0.1781(18)	0.1838(9)	0.1819(10)	0.1856(4) [8e]
O (24g) x	0.3556(7)	0.35775(24)	0.3522031)	0.3542(4)/0.3531(4) [24i]
z	0.0408(8)	0.4104(23)	0.04180(32)	0.056(2) [24i]
Thermal displacement parameters $U_i/U_{eq} \times 100$/Å^2				
T	2.73(35)	2.23(13)	4.95(23)	—
O	1.85(15)	1.01(7)	2.52(6)	—
Na	7.5(12)	15.07[b]	15.69(10)	—
Br	3.0(6)	2.10(16)	1.48(22)	—
Derived bond lengths/angles				
Na–Br/Å	2.734(13)	2.786(13)	2.771(15)	2.872(8)
Na–O/Å	2.466(8)	2.490(6)	2.450(4)	2.363(1)
	3.160(8)	3.170(6)	3.193(10)	3.024(7)
T–O/Å	1.5996(14)	1.6030(6)	1.6223(13)	1.670(7)/1.683(7)
T–O–T/°	148.8(4)	149.77(17)	146.76(30)	140.43(12)

[a] Data taken from the Inorganic Chemical Structural Database. [b] Anisotropic thermal displacement parameters modelled with U_{eq} values given and refine values (U_{11}, $U_{22}\cdots$) $\times 100$ as 15.1(6) 15.1(6) 15.1(6) −0.5(6) −0.5(6) −0.5(6).

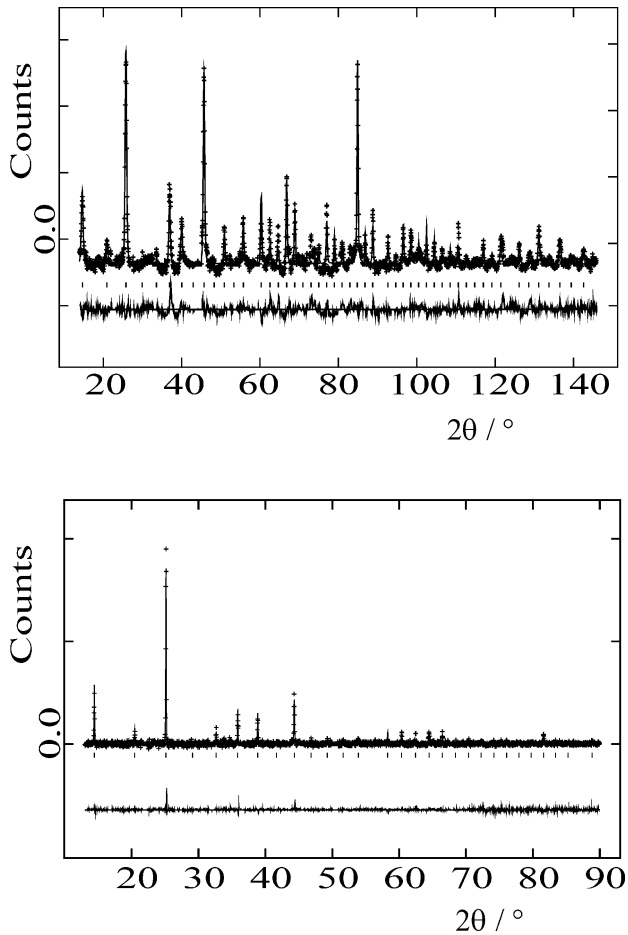

Fig. 2 Typical X-ray (upper) and neutron diffraction (lower) profile fits using data from $Na_8[Si_8Be_2Al_2O_{24}]Cl_2$, crosses are observed data, upper continuous line the calculated profile, lower continuous line the difference. Tick marks show reflection positions.

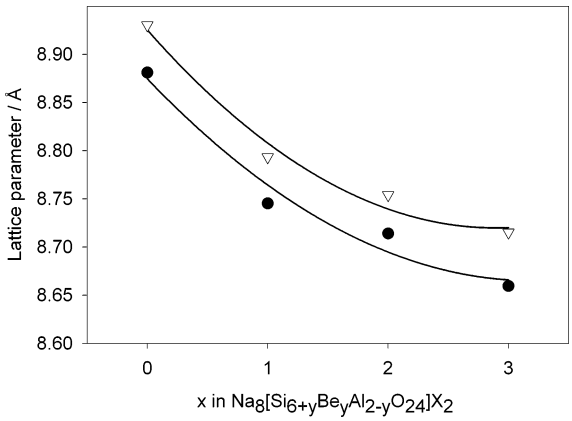

Fig. 3 Variation of the lattice parameter as a function of y in $Na_8[Si_{6+y}Be_yAl_{2-y}O_{24}]X_2$, X = Cl, Br. (●) X = Cl and (▽) X = Br.

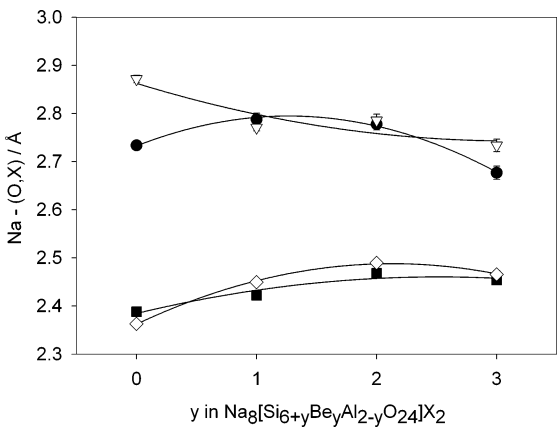

Fig. 4 Variation of the Na–O and Na–Cl, Br distances in $Na_8[Si_{6+y}Be_yAl_{2-y}O_{24}]Cl_2$ as a function of y. (●) and (◇) X = Cl; (▽) and (■) X = Br.

Fig. 4 summarises the behaviour of the extracted sodium environment as beryllium is substituted into the sodalite framework in $Na_8[Si_{6+y}Be_yAl_{6-2y}O_{24}]X_2$. These data indicate that as beryllium is incorporated there is a slight general increase in the derived Na–O distance while the average Na–X separation decreases, particularly for X = Br. Note that the measured Na–O distance, Fig. 4, reflects an average value associated with a static distribution of

sodium and oxygen atoms that in turn results from the specific local distribution of framework T-species in the six-ring to which the sodium ion coordinates though the oxygen. This distribution is translated into the anomalously high thermal displacement parameters associated with these two ions, particularly for the $Na_8[Si_8Be_2Al_2O_{24}]X_2$ and $Na_8[Si_7BeAl_4O_{24}]X_2$ members with disordering of three types of T atom across the 6 T sites in this ring. The extracted Na–X, X = Cl, Br, distances are reasonable for these ion pairs though with increasing beryllium content in the framework these interactions are placed under some compression with the values decreasing slightly in $Na_8[Be_3Si_9O_{24}]X_2$ from the values in the aluminosilicate materials, Fig. 4. This decrease is not monotonic with the chloride berylloaluminosilicate materials showing an extracted, initial small increase in average Na–Cl distance; however this may just reflect the effects local atomic disorder and potentially also a local displacement of the chloride ion from the cage centre in any one sodalite cage composition.

As beryllium is incorporated into the structure with a resultant contraction in the T–O distances the framework oxygen to sodium ion distances need to be maintained at typical values for this interaction (that is in the range 2.35–2.50 Å). To accomplish this the framework tilt angle needs to increase and these behaviours can be seen in the gradual increase in the average T–O–T bond angle as y increases in the two series $Na_8[Si_{6+y}Be_yAl_{6-2y}O_{24}]X_2$, X = Cl and Br, Table 2.

The structural behaviours of the various $Na_8[Si_{6+y}Be_y$-$Al_{6-2y}O_{24}]X_2$, X = Cl and Br phases at high temperature are typical of many sodalite materials. The evolutions of the structures of natural tugtupite and synthetic chloride sodalite as a function of temperature have been studied in detail previously.[36,37] Fig. 5 summarises the thermal expansion behaviours of the materials studied in this work and of these previously investigated compounds. The slightly anomalous behaviour of natural tugtupite has been described as resulting from the rotations of the T–O tetrahedra rather than extension of the Na–O and other bond lengths and this results in fairly low expansion coefficient, with a unit cell volume change of only 3% between room temperature and 1000 K. In contrast, the unit cell volume of $Na_8[AlSiO_4]_6Cl_2$ increases by 4.8% over the same temperature range. The variable temperature data obtained in this work are more limited, but parallel the behaviour of $Na_8[AlSiO_4]_6Cl_2$ very closely. Expansion coefficients match those reported for sodalite and are distinctly larger than that of natural tugtupite—even for the analogous synthetic composition $Na_8[Si_7BeAl_4O_{24}]Cl_2$. This probably reflects the effect of framework ordering and the adoption of a tetragonal unit cell for natural tugtupite allowing a more concerted expansion of the various bond lengths present. The thermal expansion behaviour of synthetic $Na_8[Si_7BeAl_4O_{24}]Cl_2$ can be considered further by reference to Fig. 6 which plots key structural parameters for this phase as a function of temperature. The observed lengthening of the Na–O bonds and opening of the T–O–T angle are the main originators of the overall expansion in the cell parameter and these increases are much more rapid than those found for natural tugtupite. The observed behaviour in the derived Na–Cl distance initially seems anomalous as this distance shortens on heating; however this behaviour probably reflects the use of an

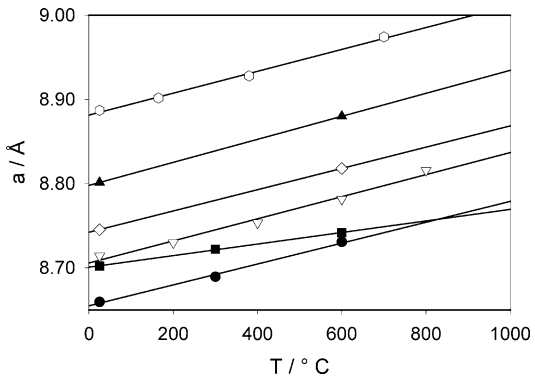

Fig. 5 Thermal expansion behaviours of $Na_8[Si_{6+y}Be_yAl_{2-y}O_{24}]X_2$ phases shown in terms of the variation of lattice parameter as a function of temperature. (●) $Na_8[Si_9Be_3O_{24}]Cl_2$, (▽) $Na_8[Si_8Be_2Al_2O_{24}]Cl_2$, (■) natural tugtupite from ref. 36) (value plotted is $V^{1/3}$ to allow direct comparison), (◇) $Na_8[Si_7BeAl_4O_{24}]Cl_2$, (▲) $Na_8[Si_7BeAl_4O_{24}]Br_2$ and (⬡) $Na_8[Si_6Al_6O_{24}]Cl_2$ from ref. 37.

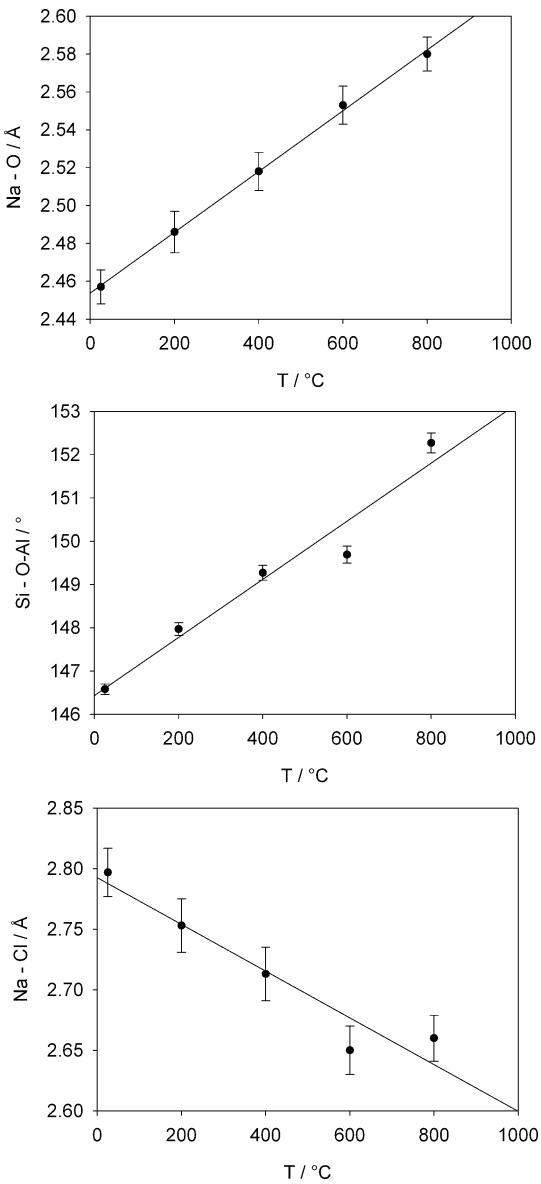

Fig. 6 Variation of key structural parameters as a function of temperature for the synthetic tugtupite analogue $Na_8[Si_7BeAl_4O_{24}]Cl_2$.

"averaged" structural model to represent the sodium ion positions. At high temperatures, the combination of static disorder and large thermal motion is well represented by a high thermal displacement parameter (TDP) and single sodium and chloride ion positions. However, at room temperature the positional disorder is less well represented by single ion sites and larger TDPs, the combination of which seems to effectively over estimate the Na–Cl distance at 298 K.

Infra-red spectra

All the new synthetic beryllium-containing frameworks showed IR spectra typical of the sodalite framework, Table 3. Previous studies of the sodalite compositions with ordered frameworks show that of the 14 modes that are active, only 6 or 7 are generally observed as reasonable intensity modes in the infrared spectrum between 400 and 1000 cm^{-1}.[38,39] More specifically a broad and very strong absorption near 1000 cm^{-1} (sometimes resolvable as two peaks) is associated with symmetric type T–O–T stretches, a series of modes between 600 and 700 cm^{-1} designated as T–O–T asymmetric stretches and 1 or 2 modes at around 460 cm^{-1} assigned as deformations. These absorptions are all observed for the series of compounds $Na_8[Si_{6+y}Be_yAl_{6-2y}O_{24}]X_2$, X = Cl, Br, produced in this study.

Previous work has correlated the exact positions of the absorptions with structural parameters such as the unit cell constant, T–O distances and T–O–T bond angles. In general, a shortening of the T–O distances and tightening of the T–O–T bond angles in framework compounds results in the asymmetric and symmetric stretching frequencies shifting to high wavenumbers.[38] This behaviour is observed and extended in the compounds produced and studied in this work. Hence replacement of aluminium by silicon and beryllium (2Al = Si + Be) results in a decrease in the average T–O distance from 1.67 Å (in sodalite, $Na_8[Si_6Al_6O_{24}]Cl_2$) to near 1.60 Å in $Na_8[Si_9Be_3O_{24}]Cl_2$ and the average T–O–T bond angle increases in a similar fashion between the two end member compounds by approximately 9 degrees for both chloride and bromide series (Tables 1 and 2). As a result of these changes in structure all the observed vibrational frequencies shift to higher wave-numbers with the most marked shifts occurring for the stretching modes. Thus the strong absorption from the asymmetric mode shifts from 984 cm^{-1} in $Na_8[Al_6Si_6O_{24}]Cl_2$ to 1047 cm^{-1} in $Na_8[Be_3Si_9O_{24}]Cl_2$. This behaviour extends that observed for other materials from the $Na_8[T_{12}O_{24}]X_2$ families. So, for example, the asymmetric stretching frequency, associated with the four rings in the sodalite cage, can be plotted smoothly as a function of average T–O distance (Fig. 7) and the T–O–T angle (Fig. 8) for various T atoms. These plots significantly extend the trends previously found for sodalite structures to the smaller frameworks containing beryllium allowing, for example, framework structural parameters to be readily estimated from simply obtained infra-red spectrum.

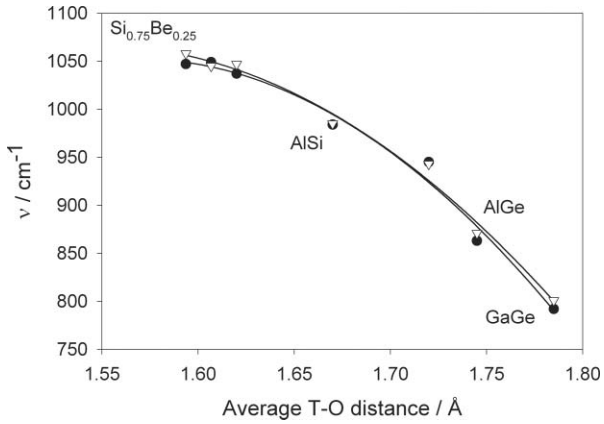

Fig. 7 Variation of the frequencies of the main infrared absorptions observed for sodalites $M_8[T,T',T''O_2]_{12}X_2$ as a function of the average T–O distance. (●) X = Cl and (▽) X = Br. For the new compositions studied in this work $Na_8[Si_{6+y}Be_yAl_{2-y}O_{24}]X_2$ $y = 1, 2, 3$ the points in the top left hand corner represent $y = 1$ to $y = 3$ from right to left.

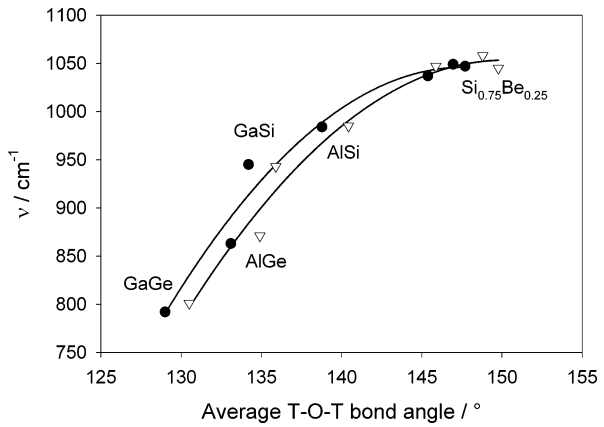

Fig. 8 Variation of the frequencies of the main infrared absorptions observed for sodalites $M_8[T,T',T''O_2]_{12}X_2$ as a function of the average T–O–T bond angle. (●) X = Cl and (▽) X = Br. For the new compositions studied in this work $Na_8[Si_{6+y}Be_yAl_{2-y}O_{24}]X_2$ $y = 1, 2, 3$ the points in the top right hand corner represent $y = 1$ to $y = 3$ from left to right.

Table 3 Main infrared vibrational frequencies (cm^{-1}) for the beryllium containing sodalite frameworks

Mode	Na_8-$[Al_6Si_6O_{24}]$-Cl_2	Na_8-$[Al_4BeSi_7O_{24}]$-Cl_2	Na_8-$[Al_2Be_2Si_8O_{24}]$-Cl_2	Natural pink tugtupite	Na_8-$[Be_3Si_9O_{24}]$-Cl_2	Na_8-$[Al_6Si_6O_{24}]$-Br_2	Na_8-$[Al_4BeSi_7O_{24}]$-Br_2	Na_8-$[Al_2Be_2Si_8O_{24}]$-Br_2	Na_8-$[Be_3Si_9O_{24}]$-Br_2
ν_{AS}	984 (vs)	1037	1048	1045	1047	985	1047	1045	1058
	960 (s)	967	977	978	982		983	983	985
ν_S	734	759	759	782	758	732	756	758	754
	712		718	753	733	708	710	728	731
	667	671	668	724	651	664	665	708	
				652			603	665	
				614				600	600
δ(O–T–O)	466		471	470	479	465	471	475	477

Discussion

A synthetic analogue of the natural semi-precious mineral tugtupite, $Na_8[Si_8Be_2Al_2O_{24}]Cl_2$, has been synthesised and the general series of berylloaluminosilicate sodalites of the general formula $Na_8[Si_{6+y}Be_yAl_{6-2y}O_{24}]X_2$, with X = Cl, Br and y = 1,2,3, also produced. Materials of the composition $Na_8[Si_9Be_3O_{24}]Cl_2$ are the first beryllosilicate frameworks with a Si : Be ratio of 3 : 1 to be synthesised. All these materials adopt the sodalite structure with a berylloaluminosilicate framework encapsulating sodium and halide ions within the standard sodalite cage, Fig. 1. The framework in all these synthetic sodalites has a disordered arrangement of tetrahedral species in contrast to natural tugtupite with its ordered Be, Al and Si sites; this difference presumably results from differences in the conditions under which the materials were formed. A high-temperature direct reaction was successful in this work, which contrasts with hydrothermal conditions under which the natural material is generated.[27] In addition the use of pure metal halide results in a white tugtupite in contrast to the natural material, which is usually pink due to the presence of sulfur species in some sodalite cages.

The disordered nature of the framework is confirmed by the ^{29}Si MASNMR spectrum obtained from $Na_8[Si_8Be_2Al_2O_{24}]Cl_2$ which shows a broad resonance centred on −94 ppm, Fig. 9. While this chemical shift is similar to that observed for the single peak from natural tugtupite (with reported values of −95.1 ppm[40] and −91.34 ppm,[41] these resonances for the natural materials are very sharp (~70 Hz). The broad resonance, halfwidth ~20 ppm, reflects a variety of Si(–OT)$_4$ environments with T = Si, Be, Al and based on previous studies of silicon containing sodalites resonances in the range Si(–OSi)$_4$, −110 ppm; Si(–OAl)$_4$, −78 ppm; and Si(–OBe)$_4$ −68 ppm[42,43] the observed spectrum is consistent with the fully disordered framework, confirming the diffraction study results. This difference between the natural and synthetic samples of composition $Na_8[Si_8Be_2Al_2O_{24}]Cl_2$ in terms of distribution of framework T sites is probably a result of the different synthesis conditions. Natural tugtupite forms in hydrothermal veins under high pressure and such conditions are likely to promote slow crystal growth and an ordered framework. Similar differences are seen between synthetic and natural (Lapis Lazuli) ultramarines where the natural material has an ordered arrangement of silicon and aluminium (space group $P\bar{4}3n$) while commercially produced $Na_8[SiAlO_4]_6(S_3)_n$ has a totally disordered framework whose structure is described in $I\bar{4}3m$.[34] One further difference is that natural tugtupites contain significant levels of various additional species such as sulfur and lanthanum and these may help direct framework ordering; indeed some preliminary work incorporating sulfate into the tugtupite framework, *i.e.* $Na_8[Si_8Be_2Al_2O_{24}](Cl_{1.8}, (SO_4)_{0.1})$, shows the formation of a tetragonal phase.

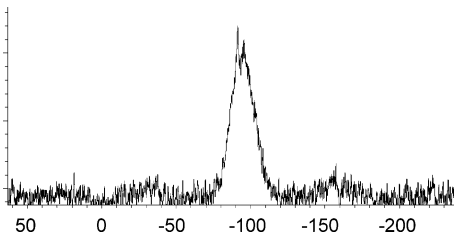

Fig. 9 ^{29}Si MASNMR spectrum obtained from $Na_8[Si_8Be_2Al_2O_{24}]Cl_2$.

The incorporation of beryllium into the sodalite structure, on the basis of 2Al → Be + Si results in the expected changes in framework geometry as the smaller Be^{2+} and Si^{4+} (Be/Si–O ~ 1.60 Å) replaces Al^{3+} (Al–O ~ 1.73 Å). Thus the average T–O distance decreases and this causes the framework tetrahedra to tilt in order to maintain the co-ordination to the extra-framework cations. The temperature dependence of the structure of natural tugtupite has previously been studied in detail[37] and shows some anomalous behaviours associated with a slower than expected expansion as the ordered framework tetrahedra are able to rotate to different levels on their individual sites to accommodate the general thermal expansion in the bond lengths. The thermal expansion behaviour of synthetic tugtupite $Na_8[Si_8Be_2Al_2O_{24}]Cl_2$ with a disordered framework is similar to that of other sodalites.

Conclusions

Synthetic berylloaluminosilicates of the general formula $Na_8[Si_{6+y}Be_yAl_{6-2y}O_{24}]X_2$, X = Cl, Br, y = 1, 2, 3, can be synthesised and their sodalite structures and structural behaviours are those expected based on the size of the tetrahedral species. However, unlike the one known natural member of this series, tugtupite, the framework is disordered as shown by diffraction and NMR studies. Further investigations will centre on the incorporation of other cationic and anionic species into these beryllium-containing frameworks in order to induce specific properties; for example a synthetic analogue of the coloured, fluorescent and photochromic natural tugtupite is sought.

The potential exists for developing numerous new framework structures incorporating BeO_4 units with the increased flexibility this species brings, first through the similarity in size of the silicate and beryllate tetrahedra and secondly through the involvement of a more highly charged framework unit, $[Be(O_4)_{1/2}]^{2-}$. This latter aspect facilitates control of the non-framework species with for example incorporation of higher levels of monovalent cations or divalent cations.

Acknowledgements

We thank Drs Paul F. Henry (ILL) and Richard M. Ibberson (ISIS) for help with the collection of the neutron diffraction data and Dr Sandie Dann (Loughborough University) for collection of the MASNMR spectrum. We also acknowledge the support of EPSRC under grant GR/S98580/01.

References

1 M. T. Weller, *Dalton Trans.*, 2000, 4227.
2 T. B. Reed and D. W. Breck, *J. Am. Chem. Soc.*, 1956, **78**, 5972.
3 Ch. Baerlocher and W. M. Meier, *Helv. Chim. Acta*, 1969, **52**, 1853.
4 K. Fischer and V. Schramm, *Adv. Chem. Ser.*, 1971, **101**, 250.
5 P. A. Cocks and C. G. Pope, *Zeolites*, 1995, **15**, 701.
6 I. Hassan, *Kuwait J. Sci. Eng.*, 1997, **24**, 163.
7 O. V. Petersen, G. Giester, F. Brandstatter and G. Niedermayr, G, *Can. Mineral.*, 2002, **40**(1), 173.
8 A. Y. Malinovskii and N. V. Belov, *Dokl. Akad. Nauk SSSR*, 1980, **252**, 611.
9 M. T. Weller and G. Wong, *Solid State Ionics*, 1989, **32 & 33**, 430.
10 M. R. M. Jiang and M. T. Weller, *Solid State Ionics*, 1991, **46**, 341.
11 M. T. Weller and G. Wong, *Eur. J. Solid State Inorg. Chem.*, 1989, **26**, 619.
12 L. Pauling, *Z. Kristallogr.*, 1930, **74**, 213.

13 P. J. Mead and M. T. Weller, *Zeolites*, 1995, **15**, 561.
14 M. T. Weller and K. E. Haworth, *J. Chem. Soc., Chem. Commun.*, 1991, 734.
15 W. Depmeier, *Acta Crystallogr., Sect. B: Struct. Sci.*, 1984, **40**, 185.
16 S. E. Dann, P. J. Mead and M. T. Weller, *Inorg. Chem.*, 1996, **35**, 1427.
17 H. Mueller-Buschbaum and J.-P. Werner, *Z. Naturforsch., B: Anorg. Chem. Org. Chem.*, 1997, **52**, 449.
18 G. M. Johnson and M. T. Weller, *Prog. Zeolite Microporous Mater.*, 1997, **105**, 269.
19 V. N. Kanepit, Y. Z. Nozik and L. E. Fykin, *Geokhimiya*, 1984, **4**, 577.
20 X. H. Bu, P. Y. Feng, T. E. Gier, D. Y. Zhao and G. D. Stucky, *J. Am. Chem. Soc.*, 1998, **120**, 13389.
21 I. Hassan and H. Grundy, *Am. Mineral.*, 1985, **70**, 186.
22 R. Kondo, *J. Ceram. Soc. Jpn.*, 1965, **73**, 1.
23 R. J. H. Clark, *Chem. Soc. Rev.*, 1999, **28**, 75.
24 I. F. Chang, *J. Electrochem. Soc., Solid State Sci. Technol.*, 1974, **121**(6), 815.
25 D. B. Medved, *Am. Mineral.*, 1954, **39**(7–8), 615.
26 M. Danø, *Acta Crystallogr.*, 1966, **20**, 812.
27 A. Jensen and O. V. Petersen, *Gems & Gemology*, The Gemological Institute of America, Carlsbad, CA, summer edn, 1982, p. 90.
28 T. E. Gier and G. D. Stucky, *Nature*, 1991, **349**, 508.
29 G. Harvey, C. Baerlocher and T. Wroblewski, *Z. Kristallogr.*, 1992, **201**(1–2), 113.
30 H. Y. Zhang, L. H. Weng, Y. M. Zhou, Z. X. Chen, J. Y. Sun and D. Y. Zhao, *J. Mater. Chem.*, 2002, **12**(3), 658.
31 W. T. A. Harrison, T. E. Gier, K. L. Moran, J. M. Nicol, H. Eckert and G. D. Stucky, *Chem. Mater.*, 1991, **3**(1), 27.
32 W. T. A. Harrison, *Acta Crystallogr. Sect., C: Cryst. Struct. Commun.*, 2001, **57**(8), 891.
33 M. A. Simonov, Yu. K. Egorov-Tismenko and N. V. Belov, *Dokl. Akad. Nauk SSSR*, 1975, **225**, 1319.
34 S. E. Tarling and P. Barnes, *Acta Crystallogr., Sect. B: Struct. Sci.*, 1988, **B44**, 128–135.
35 B. Beagley, C. M. B. Henderson and D. Taylor, *Mineral. Mag.*, 1982, **46**, 459.
36 I. Hassan and H. D. Grundy, *Can. Mineral.*, 1991, **29**, 385.
37 I. Hassan, S. M. Antao and J. B. Praise, *Am. Mineral.*, 2004, **89**(2–3), 359.
38 C. M. B. Henderson and D. Taylor, *Spectrochim. Acta, Part A*, 1979, **35**, 929.
39 J. Godber and G. A. Ozin, *J. Phys. Chem.*, 1988, **92**, 4980.
40 Z. Xu and B. L. Sherriff, *Can. Mineral.*, 1994, **32**, 935.
41 J. Skibsted, P. Norby, H. Bildsøe and H. J. Jakobsen, *Solid State Nucl. Magn. Reson.*, 1995, **5**, 239.
42 M. T. Weller, S. E. Dann, G. M. Johnson and P. J. Mead, *Prog. Zeolite Microporous Mater.*, 1997, **105**, 455.
43 S. E. Dann and M. T. Weller, *Solid State Nucl. Magn. Reson.*, 1997, **10**, 89.